https://doi.org/10.5194/bg-2023-95
Preprint. Discussion started: 1 August 2023

Biogeosciences Discussions

Synergistic use of Sentinel-2 and UAV-derived data for Plant Community Cover distribution mapping of coastal meadows with Digital Elevation Models.

Ricardo Martínez Prentice[1], Miguel Villoslada Peciña[1,2], Raymond D. Ward[1,3], Thaisa F.Bergamo[1,2], Chris B.Joyce[3], and Kalev Sepp[1]

[1]Institute of Agriculture and Environmental Sciences, Estonian University of Life Sciences, Kreutzwaldi 5, EE-51006 Tartu, Estonia
[2]Department of Geographical and Historical Studies, University of Eastern Finland, P.O. Box 111, 80101 Joensuu, Finland
[3]Centre for Aquatic Environments, School of Applied Sciences, University of Brighton, Cockcroft Building, Moulsecoomb, Brighton BN2 4GJ, UK

Correspondence: Ricardo Martínez Prentice (ricardo@emu.ee)

Abstract. Coastal wetlands provide a range of ecosystem services, yet are currently under threat from global change impacts. Thus, monitoring and assessment is vital for evaluating their status, extent and distribution. Remote sensing provides an excellent tool for evaluating coastal ecosystems, whether with small scale studies using drones or national/regional/global scale studies using satellite derived data. This study used a fine-scale plant community classification of coastal meadows in Estonia derived from a multispectral camera on board Unoccupied Aerial Vehicles (UAV) to calculate the Plant Fractional Cover (PFC) in Sentinel-2 MultiSpectral Instrument sensor (MSI) grids. A Random Forest algorithm was trained and tested with vegetation indices (VI) calculated from the spectral bands extracted from the MSI sensor to predict the PFC. Additional RF models were trained and tested after adding a Digital Elevation Model (DEM). After comparing the models, results show that using DEM with VI can increase the prediction accuracy of PFC up to two times (R^2 58-70%). This suggests the use of ancillary data such as DEM to improve the prediction of empirical machine learning models, providing an appropriate approach to upscale local studies to wider areas for management and conservation purposes.

1 Introduction

Vegetation is the main target of study to monitor ecosystem change caused by drastic environmental shifts, because it is the key structural component of ecosystems (Díaz-Delgado et al., 2019b; Van der Maarel, 2005). Variations in the distribution patterns of vegetation over an area depend on climate, environmental factors and human activities (Gardner et al., 2009) and can be assessed by identifying plant communities. These are assemblages of plant species at a place and time (Magurran, 1988; Spiegelberger et al., 2012), and are considered as ecosystem service (ESs) - providing units, as their structure and function directly underpins the supply of ESs (Luck et al., 2003; Burkhard et al., 2012).

Traditional in-situ field survey methods have played a key role in studying spatio-temporal patterns in plant community distribution, environmental monitoring, and biodiversity conservation (Chytry et al., 2011). However, as the growing impacts

https://doi.org/10.5194/bg-2023-95
Preprint. Discussion started: 1 August 2023

of land-use intensification and climate change become more conspicuous and widespread (Findell et al., 2017), local-scale field survey methods may not adequately reveal plant community shifts in a spatially-explicit manner. Tools such as remote sensing in combination with artificial intelligence are essential to supply comprehensive assessments of these shifts (Knight et al., 2006; Adam et al., 2010; Pettorelli et al., 2014).

Remote Sensing has played a key role in wetland mapping, monitoring and trend detection, overcoming some of the difficulties of wetland survey, such as the large areal extents, remoteness and inaccessibility (Mahdianpari et al., 2020). Wetlands are one of the most degraded type of ecosystems in the world and natural wetlands have experienced a 50% decline in total area since 1900 (Davidson, 2014), continuing to decline by 35% between 1970 and 2015, mainly due to agricultural expansion and intensification, and drought (Courouble, 2021). Among wetlands, coastal wetlands have increasingly received attention due to their capacity for carbon sequestration (Hopkinson et al., 2012; Ward, 2020), coastal protection (Gedan et al., 2011) and biodiversity maintenance (Sutton-Grier and Sandifer, 2019).

Boreal Baltic coastal meadows, as stated in Annex I of the EU Habitats Directive (1992), are semi-natural wetlands managed for centuries with low-intensity activities (Paal, 1998) such as grazing and mowing. Many such meadows along the Baltic Sea coast currently show a degraded ecological status as a consequence of agriculture intensification or abandonment of traditional management (Henle et al, 2008, Rannap et al, 2004). Since the 1960s, the total area of coastal meadows has decreased by 34000 ha in Estonia, affecting a range of breeding and migratory bird species listed in the Birds Directive (Rannap et al, 2004, Leito et al, 2014). To assess the effectiveness of conservation efforts, previous studies on coastal meadows have focused on the effects of different environmental and management factors on the distribution of plant communities, such as microtopography (Ward et al, 2016a), grazing abandonment (Burnside et al, 2007), mowing (Berg et al., 2012), and sea level rise (Ward et al., 2016).

Remote Sensing techniques are increasingly used to map the distribution of coastal meadow plant communities (Villoslada et al., 2020; Martínez Prentice et al., 2021) and to estimate biomass and sward structure using Unoccupied Aerial Vehicles (UAVs) (Villoslada Peciña et al., 2021). The very high spatial resolutions supplied by UAV-borne sensors also allow fine-grained ecosystem properties to be unveiled that remain concealed under the coarse spatial resolution of satellites, such as plant fractional cover, soil organic carbon, or aboveground biomass (Heil et al., 2022). In addition, near-real-time monitoring routines and the avoidance of the effect of clouds are among the advantages of UAVs over satellite sensors (Colomina and Molina, 2014; Díaz-Delgado et al., 2019a). Conversely, the disadvantages are not only their limited coverage and battery capacity but also the legislation restrictions and their dependency on the weather conditions, as well as the requirement to be in the field (Cracknell, 2017; Emilien et al., 2021).

On the other hand, Earth Observation satellites capture images with large swaths and a high temporal resolution, which allows the consistent study of large extents of ecosystems over multiple years. In the last decade, the idea of combining the high spatial resolution derived from UAVs with the large swath and regular revisit times of satellites has gained momentum. Some studies have successfully addressed the potential upscaling of UAV multispectral images to satellite image resolutions in order to address wetland biophysical variables at multiple scales (Laliberte et al., 2011; Díaz-Delgado et al., 2019a) with

https://doi.org/10.5194/bg-2023-95
Preprint. Discussion started: 1 August 2023

UAV as a support for ground-truth observations. The accurate geometrical and radiometrical overlapping allows UAV imagery values to be aggregated into satellite pixel grids (Padró et al., 2018).

Modelling plant community coverage with remote sensing data is one of the main goals in ecological assessments and monitoring (Corbane et al., 2015). Combining remotely sensed data with Machine Learning (ML) algorithms shows robust performance due to their ability to deal with non-parametric distribution of the ground-truth data as well as the multicollinearity of variables (Rodriguez-Galiano et al., 2012; E Thessen, 2016; Maurya et al., 2021). ML-based models are used to predict the presence of vegetation using indices as the input for different algorithms (Maurya et al., 2021), and Random Forest (RF) has been shown to be an accurate algorithm to predict Plant Fractional Cover (PFC) over large areas (Zhang et al., 2019; De Simone et al., 2021). Moreover, ancillary data such as Digital Elevation Models (DEM) interpolated from Light Detection and Ranging (LiDAR) point clouds have been successfully used for mapping plant communities in coastal wetlands (Ward et al., 2013) together with multispectral data from remote sensing platforms. This combination provides an enhancement on the detection of new plant distribution patterns (Okolie and Smit, 2022).

The present study compared two PFC models of five plant communities in Estonian coastal meadows from spectral indices calculated with Sentinel-2 MultiSpectral Instrument (MSI) sensor and ancillary data from a DEM. High-resolution UAV imagery was used as the reference for PFC within the spatial resolution of a Sentinel-2 image. The main objectives were to: (1) quantify the relationship between UAV imagery and MSI imagery values; (2) predict and test ML models to predict individual PFC per plant community with VI derived from Sentinel-2 spectral values; (3) predict and test the performance of the models by adding DEM data to the VI.

2 Materials and Methods

2.1 Study areas

Six coastal meadow study sites located in protected areas on the west coast of Estonia were selected for this study. Kudani (KUD), Tahu North (TAN) and Tahu South (TAS) belong to the Silma Nature Reserve; Rälby (RAL) and Rumpo East (RUE), to the Vormsi Landscape Protection Area; and Matsalu (MAT), to the Matsalu National Park (Figure 1). These landscapes are characterized by coastal meadows extended over a gradual transition from the sea to terrestrial ecosystems with a low variation of topography, typically 0 to 2 metres above mean sea level (Ward et al., 2016). Sites were chosen based on their near-continuous management history, high conservation value for wading birds, and presence of endangered plant species (Rannap et al., 2004; Berg et al., 2012).

The plant communities under study are very characteristic of Estonian coastal meadows and have been previously grouped following a phytosociological classification by Burnside et al (2007): Lower Shore (LS), Open pioneer (OP), Upper shore (US), Tall grassland (TG), and Reed Swamp (RS). This classification has been used in various studies in these coastal meadows and the plant communities have proven to be differentiable from high-resolution images (ca. 10 centimetres per pixel) (Ward et al., 2013; Villoslada et al., 2020; Martínez Prentice et al., 2021). The distribution of plant communities shows site-specific patterns

https://doi.org/10.5194/bg-2023-95
Preprint. Discussion started: 1 August 2023

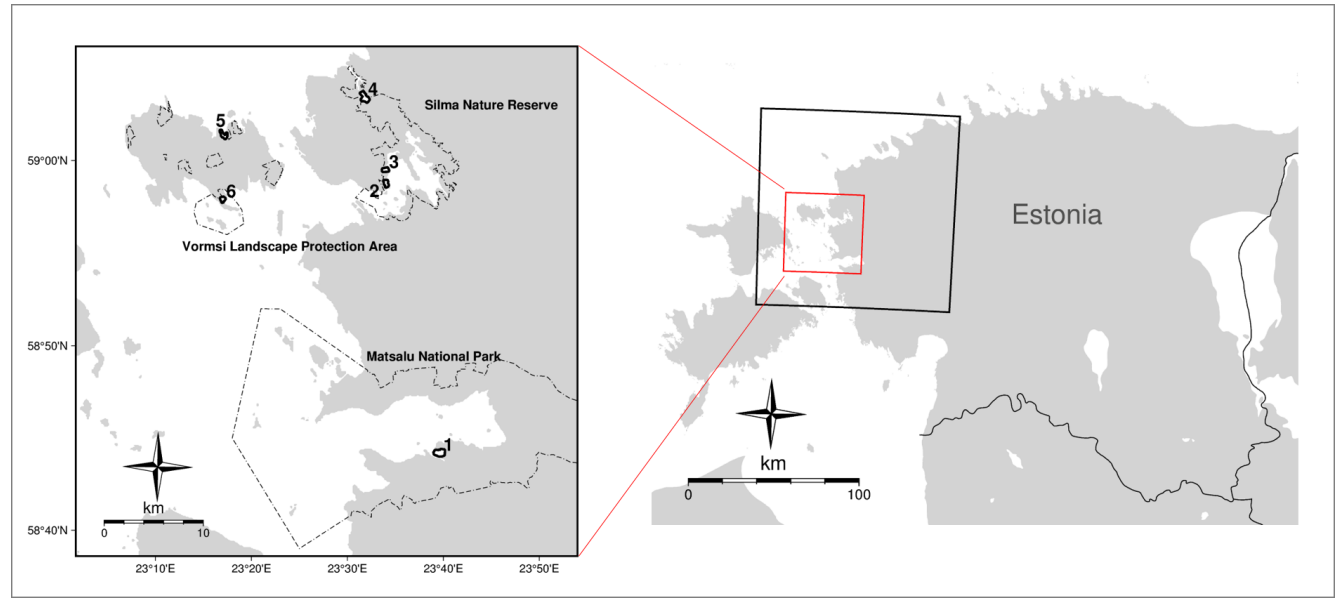

Figure 1. Location of the study sites in the western coast of Estonia. 1. Matsalu, 2. Tahu South, 3. Tahu North, 4. Kudani, 5. Rälby, 6. Rumpo. The black square shows the Sentinel-2 tile footprint, whereas the extent of all the study areas is in red.

2.2 UAV classification data

A classification of the plant communities from high-resolution images (Martínez Prentice et al., 2021) was used as the training/validation data in the present study. A multispectral Parrot Sequoia (PS) camera was carried on board of an eBee fixed-wing drone controlled remotely with the software SenseFly eMotion (Parrot S.A. Paris) over the six study areas at an altitude of 120 m to obtain Ground Sample Distance of 10 cm. Flight dates are shown in Table 1. The images were radiometrically corrected with Airinov calibration panels and a sunshine sensor to produce multi band orthoimages that were merged in Pix4D v.4.3.31 software. VI were calculated based on all the spectral bands (near infrared, red edge, red and green spectral bands) and used as input for two different workflows: a pixel-based classification, where the pixels were classified with a Random Forest and K-nearest neighbours' algorithms; and segmentation for an object-based classification with the same algorithms. The highest accuracy was achieved by a Random Forest pixel classification (accuracy and kappa greater than 90% and 0.85, respectively), calculated from a confusion matrix constructed using 140 vegetation survey quadrats as training samples, where all the species with coverage above 5% were recorded within the quadrats. For the OP community all plants were recorded as a result of the low cover of all species and predominance of bare ground. Not all the plant communities were present in each site (Table A1). Further details of this methodology and results can be obtained in Prentice et al (2021).

https://doi.org/10.5194/bg-2023-95
Preprint. Discussion started: 1 August 2023


Biogeosciences Discussions Open Access EGU

2.3 Satellite imagery

Recent studies have shown that images taken by light-weight cameras in the visible and near infrared spectrum (VNIR) on board of UAV have a good correlation with satellite images, especially with MSI images of Sentinel-2 (Zabala, 2017; Zhu et al., 2021). Thus, one Sentinel-2 Level 2A image covering the six study areas (Fig. 1) with the closest date to the drone flights was used, with an estimated cloud cover of 19% (Table 1). The tile number was T34VFL and its date, 24/06/2019. The level 2A was chosen because the orthorectified Bottom-of-Atmosphere reflectance values are comparable with PS reflectance (Fawcett et al., 2020). This image product is radiometrically corrected by the Payload Data Ground Segment with Sen2Cor algorithm (Main-Knorn et al., 2017) and available online via the Copernicus Scientific Data Hub tool (Cop).

Table 1. Flight dates and tile number and date of Sentinel-2 overpass to match the drone flights

Study Area	Drone flight date
MAT	29/06/2019
TAS	23/07/2019
TAN	30/06/2019
KUD	30/06/2019
RAL	04/07/2019
RMP	02/07/2019

Band 6 from MSI is in the Red-Edge region (Table 2) and contains valuable information of vegetation, avoiding background reflectance that affects wetlands especially (Turpie, 2013). Its spatial resolution is 20 metres per pixel. To use its reflectance values with the highest spatial resolution corresponding to the VNIR bands at 10 metres, a resolution enhancement process based on a super-resolution method was applied, instead of using a panchromatic band to carry out a pan-sharpening since this band does not exist in MSI. The super-resolution algorithm (Brodu, 2017) is available in the SNAP software (ESA, 2014) and combines the geometric and radiometric information of target bands to pan-sharpen the lower resolution band.

2.4 Digital Elevation Models

DEMs constitute a powerful co-predictor in species distribution models, due to the prominent role of elevation in the distribution patterns of coastal plant communities (Ward et al., 2013). This holds especially true for coastal meadows, characterized by pronounced salinity and moisture gradients due to small variations of elevation, called microtopography (Ward et al., 2016). Thus, a high-spatial resolution DEM was included in the models to test whether prediction accuracies improved. A LiDAR-derived DEM was downloaded from Eesti Maa-amet (Ees) with a spatial resolution of 1 meter. The DEM was interpolated from a LiDAR point cloud of density of 2.1 points per square using a streaming triangulation (Isenburg et al., 2006).

https://doi.org/10.5194/bg-2023-95
Preprint. Discussion started: 1 August 2023


Biogeosciences Discussions Open Access EGU

Table 2. Comparison of spectral bands in both sensors: Multispectral Instrument on board of Sentinel-2 and Parrot Sequoia on board of eBee.

Band	Multispectral Instrument	Parrot Sequoia
Green	559.8 @35	550 @40
Red	664.6 @30	660 @40
Red Edge	740.5 @14	735 @10
Near Infrared	832.8 @105	790 @40

2.5 Image processing and upscaling

A key process to perform upscaling of remote sensing images is the aggregation of pixel values from a high-resolution image to the geographically coincident pixels of coarser resolution image. Several studies have performed the aggregation process to a common geographical data frame in the form of a quasi-continuous grid, where all the spectral data is stored (Padró et al., 2018; Riihimäki et al., 2019; Mao et al., 2022; Bergamo et al., 2023). In the present study, the grid was constrained to the limits of each study area, avoiding those overlapping with the edges, excluding transitional areas that do not correspond to the extent of plant communities of interest and submerged areas. In total, 9766 MSI pixels cover the study areas (Fig. 2).

https://doi.org/10.5194/bg-2023-95
Preprint. Discussion started: 1 August 2023

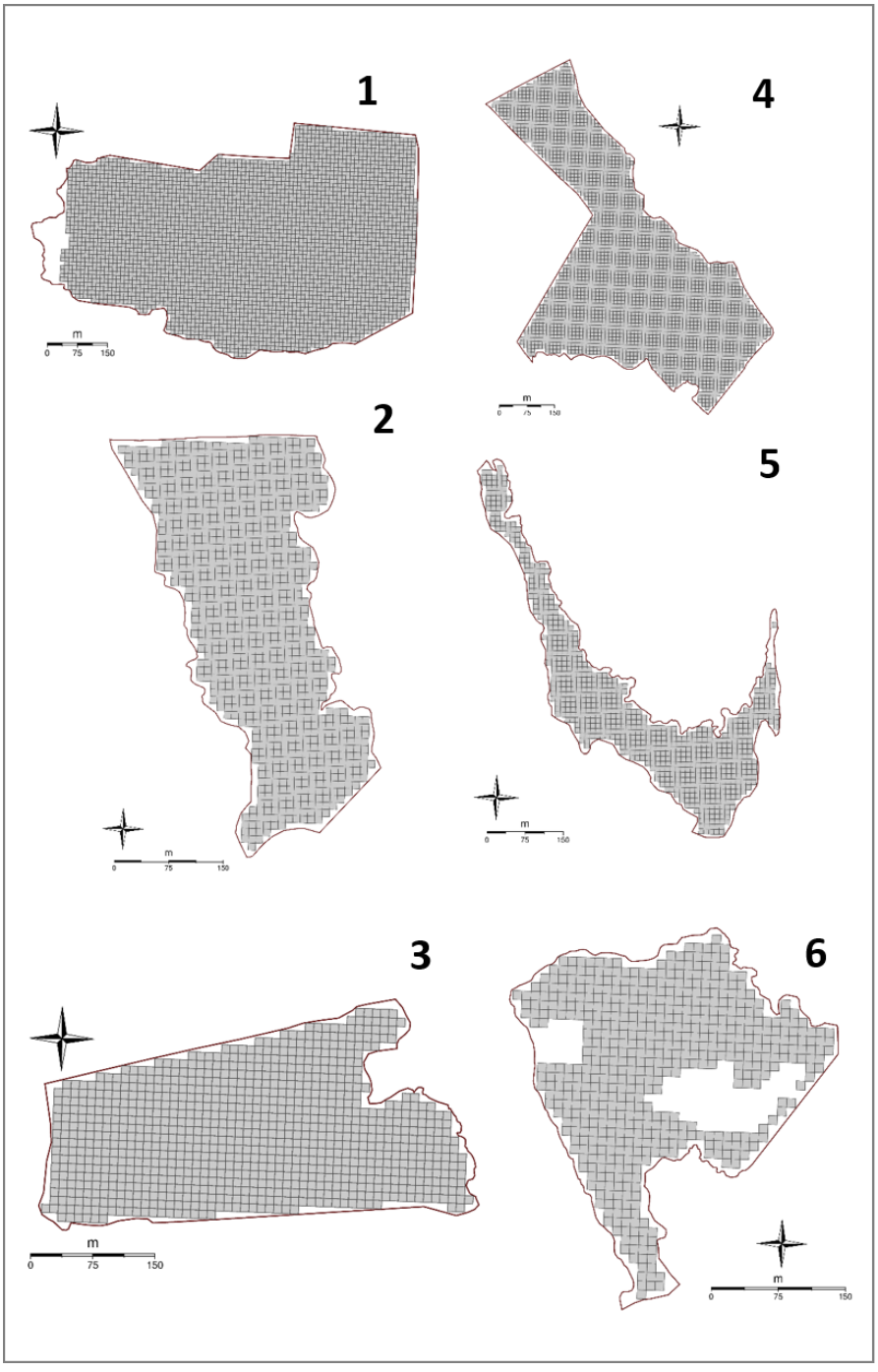

Figure 2. Data frame derived from Sentinel-2 MultiSpectral Instrument (MSI) pixels (9766) covering the six study areas. 1. Matsalu, 2. Tahu South, 3. Tahu North, 4. Kudani, 5. Rälby, 6. Rumpo.

https://doi.org/10.5194/bg-2023-95
Preprint. Discussion started: 1 August 2023

A band-to-band comparison between the PS bands used for the final classification in Prentice et al (2021) and MSI reflectance values was undertaken to assess the potential differences in both sensors caused by different temporal, spectral or spatial resolutions (Padró et al., 2018; Fernández-Guisuraga et al., 2018; Jiang et al., 2022; Isgró et al., 2022). To carry out this process, PS and MSI reflectance values were transferred into a polygon grid generated with the exact cell size as the MSI image pixels covering the study areas with an associated unique identifier (ID) for each row of the data frame (Fig. 3). Level 2A MSI reflectance values were transferred to each cell of the polygon grid and the PS values were aggregated calculating the average (Fig. 3). A correlation and a linear function were used for a band-to-band comparison, retrieving the significance level, R^2 and Root Mean Squared Error (RMSE). DEM values were integrated into the polygon grid using an average aggregation of pixels (Fig. 2) and the percentage cover of each plant community under study was calculated by intersecting the UAV-derived classification maps (Martínez Prentice et al., 2021) with the polygon grid. For all the operations, all the pixels completely covered by each grid were extracted.

https://doi.org/10.5194/bg-2023-95
Preprint. Discussion started: 1 August 2023

Biogeosciences
Discussions
Open Access
EGU

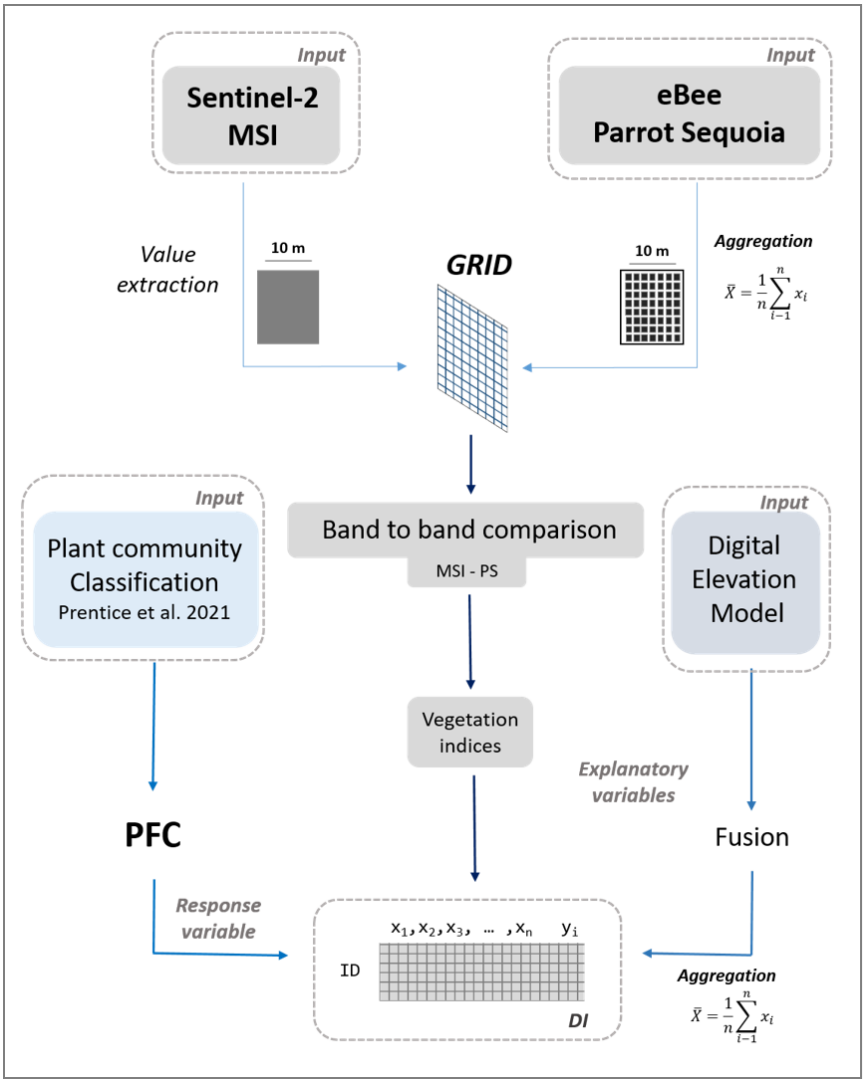

Figure 3. General workflow. The source data is marked as "Input" and the output data frame is DI. The final data frame contains the explanatory variables (x_n) and response variable (y_i) of Plant Fractional Cover (PFC), where i = Lower Shore (LS), Open Pioneer (OP), Upper Shore (US), Tall Grass (TG), Reed Swamp (RS).

The PFC was the response variable under assessment for each plant community. PFC was calculated within each MSI pixel in the main data frame after an overlay process of the classification and MSI pixel extents (equation 1). This equation was applied to each plant community of study.

$$PFC = \frac{Area\,of\,plant\,community\,within\,pixel\,extent}{Area\,of\,MSI\,pixel} \times 100 \quad (1)$$

https://doi.org/10.5194/bg-2023-95
Preprint. Discussion started: 1 August 2023

All processes were carried out using the open source Python packages NumPy (Harris et al., 2020), GeoPandas (Jordahl et al., 2020) and rasterio (Gillies, 2013).

2.6 Vegetation indices

Vegetation indices (VI) are quantitative and dimensionless mathematical combinations of spectral bands, related to vegetation structural properties (Lima-Cueto et al., 2019). VIs have been used to monitor vegetation cover by the enhancement of spectral contrast between photosynthetically active vegetation and other components (Andreatta et al., 2022). In total, 14 vegetation indices were calculated (Table 3) from all the MSI bands of this study. The red edge MSI band was included in the calculations of VI because its reflectances show the highest photosynthetical activity and thus, better differentiation between plant communities (Schuster et al., 2012; Turpie, 2013). The indices in Table 3 were calculated by combining the features in the data frame (Fig. 1) using the Pandas Python package (McKinney, 2010).

Table 3. List of fourteen vegetation indices used as explanatory variables in this study. G: Green band; R: Red band; Rre: Red Edge band; NIR: Near Infrarred band.

Vegetation Index	Calculation	Reference
Normalized Difference Vegetation Index	$NDVI = \frac{NIR-R}{NIR+R}$	(Rouse et al., 1973)
Green Normalized Difference Vegetation Index	$GNDVI = \frac{NIR-G}{NIR+G}$	(Gitelson et al., 1996)
Chlorophyll Vegetation Index	$CVI = \frac{NIR \times R}{G^2}$	(Vincini et al., 2008)
Modified Simple Ratio (red edge)	$MSRred = \frac{(NIR/Rre)-1}{\sqrt{(NIR/Rre)+1}}$	(Wu et al., 2008)
Red edge triangular vegetation index (core)	$RTVI_{\text{core}} = 100 \times (NIR - Rre) - 10 \times (NIR - G)$	(Chen et al., 2010)
Canopy Chlorophyll Content Index	$CCCI = \frac{(NIR-Rre)/(NIR+Rre)}{(NIR-R)/(NIR+R)}$	(Barnes et al., 2000)
Chlorophyll Index (red edge)	$CI_{\text{re}} = \frac{NIR}{Rre} - 1$	(Gitelson et al., 2003)
Chlorophyll Index (green)	$CI_{\text{g}} = \frac{NIR}{G} - 1$	(Merzlyak et al., 2003)
Red edge normalized difference vegetation index	$NDVI_{\text{re}} = \frac{NIR - Rre}{NIR + Rre}$	(Gitelson and Merzlyak, 1994)
Datt4	$datt_4 = \frac{R}{(G \times Rre))}$	(Datt, 1998)
Modified Green Red Vegetation Index	$MGRVI = \frac{(G^2-R^2)}{(G^2+R^2)}$	(Bendig et al., 2015)
Modified Soil Adjusted Vegetation Index	$MGRVI = \frac{2 \times NIR+1-\sqrt{(2 \times NIR+1)^2-8 \times (NIR-R)}}{2}$	(Qi et al., 1994)
Red Edge Ratio	$SR = \frac{NIR}{Rre}$	(Gitelson and Merzlyak, 1994)
Green-red vegetation index	$GRVI = \frac{G-R}{G+R}$	(Chen et al., 2019)

https://doi.org/10.5194/bg-2023-95
Preprint. Discussion started: 1 August 2023

2.7 Machine Learning models

A ML algorithm was chosen to build a PFC model because this approach has been successfully used in various ecological applications with Remote Sensing data (Olden et al., 2008; E Thessen, 2016). More specifically, the Random Forest (RF) algorithm is widely accepted because of its high performance in modelling species occurrence and distribution with remote sensing data without making assumptions of data distribution (Evans et al., 2011; Shiferaw et al., 2019; Valavi et al., 2021). This algorithm was chosen to build ten RF regression models.

To build the training and test samples, a stratified sampling from the initial data frame (DI, Fig. 3) was carried out. The values of PFC were grouped in four bins created for this purpose ('0-25', '25-50', '50-75' and '75-100'). The bin '0-25' contained the majority of PFC values in all the plant communities, causing an imbalanced distribution. This is due to the presence of minimum cover or absence of plant communities in a large share of the grid cells. Imbalanced distributions are common in ecological data (Tang et al., 2023). To account for this, an under-sampling strategy was done by reducing the number of values in each of the bins to the number of values in the minority bin (Table 4).

Table 4. Balanced training dataset per plant community with the number of training rows considered in each bin and the proportion of all the bins in relation to the number of all Sentinel-2 MultiSpectral Instrument (MSI) pixels (9766). Plant communities are: Lower Shore (LS), Open Pioneer (OP), Upper Shore (US), Tall Grass (TG), Reed Swamp (RS).

Plant	0 - 25	25 - 50	50 - 75	75 - 100	Total	Proportion (%)
LS	823	823	823	823	3292	34
OP	178	178	178	178	712	7
US	1169	1169	1169	1169	4676	48
TG	711	711	711	711	2844	29
RS	100	100	100	100	400	4

This procedure balanced the number of rows per bin, avoiding overfitting of the models on the skewed bin of values. Two models were built for each plant community (LS, OP, US, TG and RS) from the sampled data frame (DF0, Fig. 4), one trained with the list of 14 VI as explanatory variables (data frame 1, DF1, Fig. 4) and the other one adding the DEM to the explanatory variables (data frame 2, DF2, Fig. 4).

https://doi.org/10.5194/bg-2023-95
Preprint. Discussion started: 1 August 2023

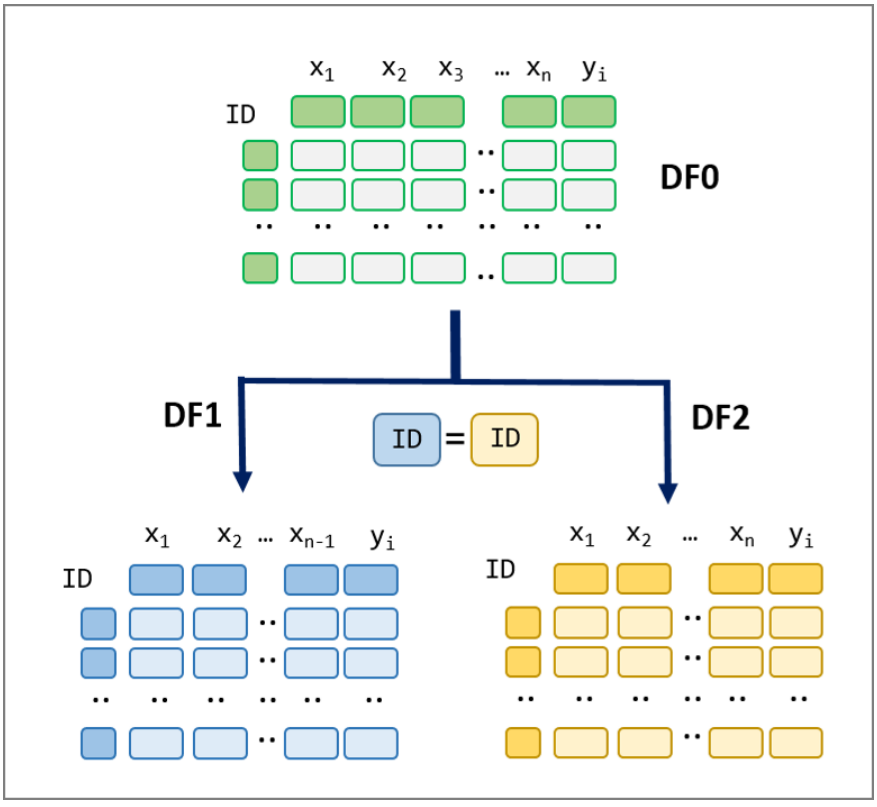

Figure 4. Diagram of the two training datasets used for the RF models per plant community. DF0 is the sampled dataset after the under-sample strategy. DF1 has the same structure as DF0 except the DEM variable (x_{n-1}) and DF2 has all the explanatory variables (x_n). y_i is the response variable (Plant Fractional Cover, PFC), where i = Lower Shore (LS), Open Pioneer (OP), Upper Shore (US), Tall Grass (TG), Reed Swamp (RS). DF1 and DF2 have the same samples (rows) matching the unique identifier (ID) column derived from DF0.

A fraction of 80% was used to train the RF regression models with DF1 and DF2 (Fig. 4). A Grid Search Cross-Validation strategy was implemented to search for the best hyperparameters and tune a RF model (Fig. 4). This method iterates through a grid of hyperparameters predefined and tests the results with a 10-fold cross validation (Fig. 4). The hyperparameters used to carry out the grid search approach were the number of estimators (N) and maximum features (MF) used to find the best split to grow each tree in the forest. The standard parameters for RF (Probst et al., 2019) were not used in this study because preliminary results did not show acceptable R^2 and RMSE scores on the training data set. The remaining 20% of the samples were used to test the trained model with the best hyperparameters. Using this approach, training and testing dependencies are removed, ensuring the robustness of the final model. In order to compare the RF models of plant communities trained with each dataset (DF1 and DF2), R^2 and RMSE metrics were reported. The models with the best scores were used to predict the fractional cover of each plant community over the whole polygon grid (Fig. 5). RF models were programmed using the package scikit-learn in Python (Pedregosa et al., 2018).

https://doi.org/10.5194/bg-2023-95
Preprint. Discussion started: 1 August 2023

Biogeosciences Discussions Open Access EGU

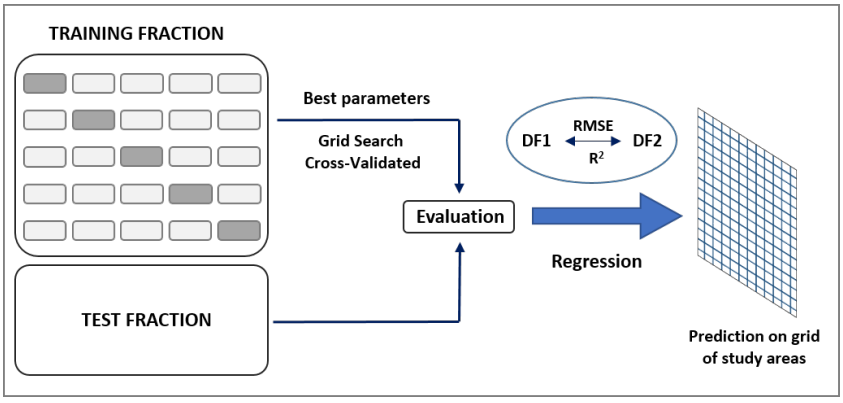

Figure 5. Machine learning algorithm training and testing process. A 10-fold cross validation on the Training fraction (80% of the input dataset) was used to search for the best hyperparameters for the Random Forest (RF) model and the 20% for Test fraction was used to test the trained model. The lowest Root Mean Square Error (RMSE) in the different RF models was used to predict the plant community distribution values on the polygon grid.

3 Results

3.1 Inter-sensor comparison

Table 5 shows a quantitative comparison of spectral overlapping bands between MS and PS with R^2, RMSE and the significance level. Although the spectral resolution of PS and MSI sensors do not overlap completely (Table 2), the PS values aggregated by average into the MSI pixel show a significant positive correlation as well as low RMSE (Table 5).

Table 5. Evaluation metrics of relations between Parrot Sequoia (PS) and Sentinel-2 Multispectral Imager sensor (MSI) spectral bands. RMSE is in reflectance units (%).

Metric	Green	Red	Red Edge	Near Infrared
R^2	56%	77%	69%	69%
RMSE	0.01	0.01	0.03	0.05
p-value	<0.05	<0.05	<0.05	<0.05

3.2 Random Forest regressions

The grid search procedure found the best model hyperparameters with a minimum of 325 N. For models built on DF1, the N were 500 except RS (325) and OP (375) and 11 MF considered for the best split. Fig. 5 shows the overall results of each RF

https://doi.org/10.5194/bg-2023-95
Preprint. Discussion started: 1 August 2023

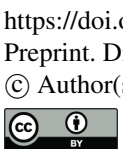

regressor model with the best hyperparameters after the Grid Search in 10-fold cross validation. The models using only the VI calculated from MSI bands (DF1) show a R^2 score under 56% and RMSE above 23% (units of PFC), resulting in a moderate to low prediction capability. Variable importance measured by the RF models do not show a common variable used to split the nodes in the models (Fig. A2). The models trained with VI and DEM values (DF2) showed a higher performance, where R^2 scores were above 58% and RMSE reduced below 22 units of PFC (Fig. 6). These models show the DEM as a common important explanatory variable used to split the nodes, except for the model to predict PFC of OP (Figures A3 and A4). Because a higher variance was explained by the models trained with DF2, they were used to predict the distribution of PFC in the whole dataset (Fig. 7).

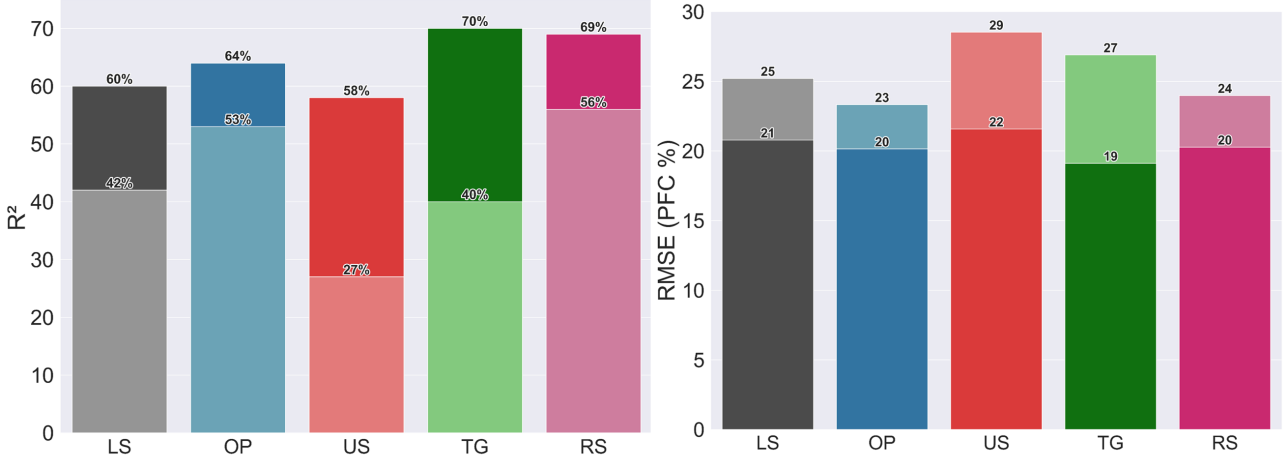

Figure 6. R^2 and Root Mean Squared Error (RMSE) retrieved by each Random Forest (RF) regressor model on plant communities. Darker shades correspond to the model scores from data frame 2 (DF2) and lighter shades are model scores from data frame 1 (DF1). Plant communities are: Lower Shore (LS), Open Pioneer (OP), Upper Shore (US), Tall Grass (TG), Reed Swamp (RS).

The best improvement of RF models is in US because the model trained and tested with VI and DEM improved its R^2 by 2.15 times more than VI alone (Fig. 6). The highest R^2 was achieved by the RF model of TG, reaching 70% after training and testing with DF2. Its RMSE decreased the most between models DF1 and DF2, from 27 to 19 units of PFC (Fig. 6). RF models trained and tested with DF1 and DF2 for LS, OP and RS show the lowest differences of R^2 and RMSE despite having 34%, 7% and 4% of the samples for training and testing.

https://doi.org/10.5194/bg-2023-95
Preprint. Discussion started: 1 August 2023

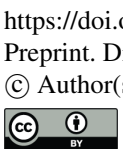

Biogeosciences
Discussions
Open Access
EGU

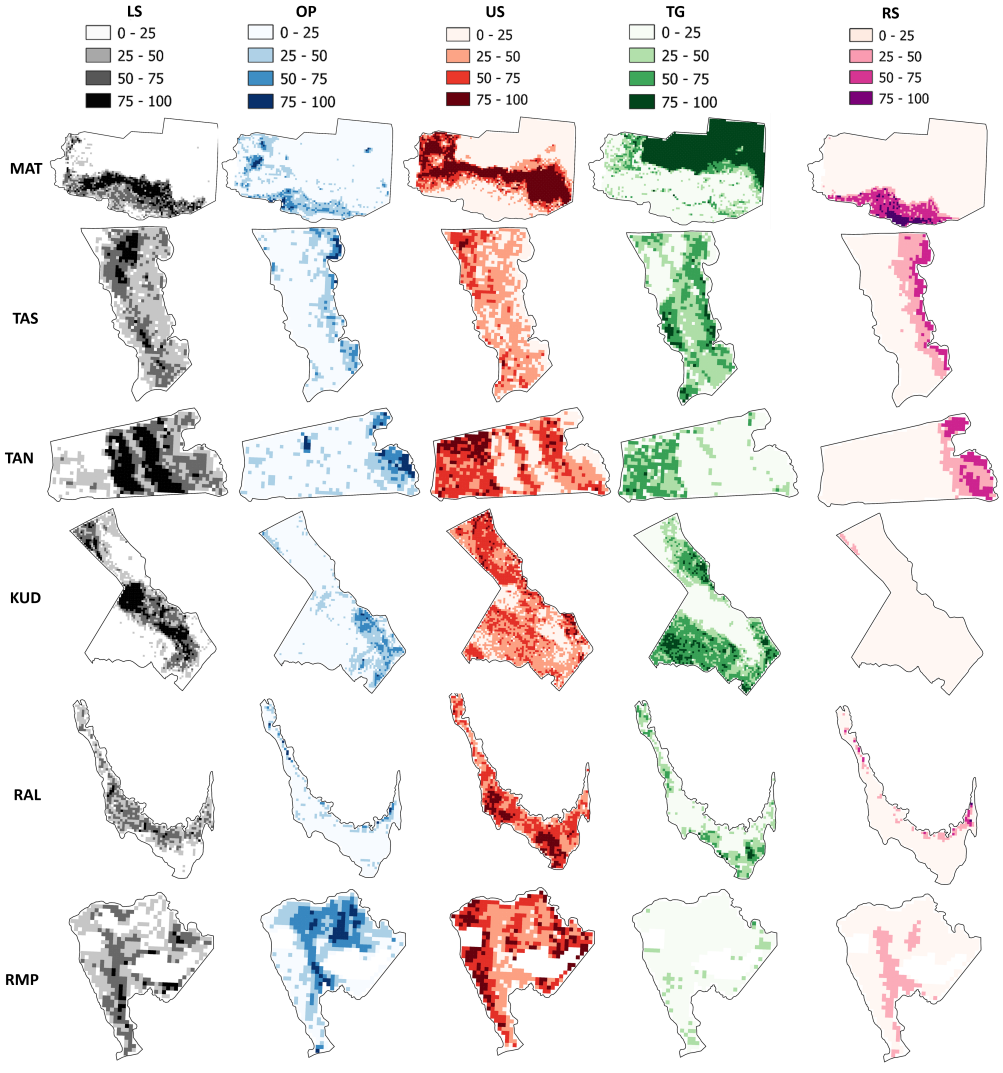

Figure 7. Maps of predicted Plant Fractional Cover (PFC ,%)for each plant community within the study areas. Lower Shore (LS), Open Pioneer (OP), Upper Shore (US), Tall Grassland (TG), Reed Swamp (RS); Matsalu (MAT), Tahu South (TAS), Tahu North (TAN), Kudani (KUD), Rälby (RAL) and Rumpo (RMP).

The prediction errors in the RF models show a scattered distribution between the predicted and real PFC (Figures A1 and A2). In general, models tend to overestimate PFC below 50% of the real value and underestimate above it, according to the differences between the best fit line of the point distribution and the identity line (perfect prediction). This is more evident on the extreme values, around 0 and 100 PFC (Figures A1 and A2). These results improve in models on DF2, which show the best-fit line closer to the identity line than those on DF1.

https://doi.org/10.5194/bg-2023-95
Preprint. Discussion started: 1 August 2023

4 Discussion

This study modelled the distribution of five coastal wetland plant communities using vegetation indices derived from the spectral bands recorded by MSI sensor and then, compared these results after the fusion of DEM data. A fine plant community classification within the study areas derived from the spectral bands of a PS camera (Martínez Prentice et al., 2021) was the reference to calculate the distribution of each plant community. Relationships between PS and MSI bands were significant after a band-to-band comparison (Table 5), making the use of this source of data comparable with the MSI reflectance values, having an average of 32% of unexplained variance in the relationships (Table 5). Similar studies compared reflectance values of PS (Díaz-Delgado et al., 2019a), or another sensor on board of UAV (Padró et al., 2018), with MSI, finding good correlations. An RF algorithm was used in this study to assess the accuracy of non-parametric based regression models to predict the distribution of plant communities, as commonly used in Earth Observation studies (Ferreira et al., 2022), due to their robustness reported in the literature (Maxwell et al., 2018). The Grid Search Cross-Validation procedure allowed the use of best model hyperparameters to construct RF regression models with the lowest errors. Each model was built on different sizes of training data sets because they were set to the minimum size of categories used per distribution (Table 4) avoiding the imbalance of minimum values of PFC (between 0-25 % of cover of each plant community). Having 48% of the total samples to train, the RF model of the US community performed the worst from DF1 values, followed by TG and LS communities, which also had a greater percentage of samples to train the models (29 and 34%, respectively, Fig. 6). These plant communities are included in a broad phytosociological categorization of grasslands (Burnside et al., 2007) with similar spatial distributions in some study areas. The mixture of reflectance signals included in one MSI pixel might have caused an overestimation of their distributions in each model. Prentice et al (2021) suggest that the presence of disagreement areas is due to a mixture of radiances in transitional areas or ecotones. The effect of mixed pixels is more significant in these types of transitional areas, as the sensor receives a wide range of reflectance signals within the extent of the pixel (Muukkonen and Heiskanen, 2007). On the other hand, RF models of OP and RS showed better results on DF1, due to their distinct ecological categorization (Burnside et al., 2007) and specific spatial distributions where there is a greater presence of water, reducing the values of VI due to lower reflectance in the Near Infrared and Red Edge spectrum. An overestimation of predicted values of these models might be due to presence of patches where plant communities were mown or trampled, thus, retrieving VI values near to bare ground values. Underestimation, on the other hand, is due to the mixture of reflectance responses from different plant communities within the same spatial distribution of MSI pixels. As shown in figures 6 and A1, all RF models improved after the fusion of high-resolution DEM (spatial resolution of 1 metre) into the spectral data (DF2, Fig. 4). Comparing the importance of variables in each model using DF1 and DF2 as shown in Fig.A2, MSAVI was the only common variable among all the models trained and tested with DF1. Once the DEM was included as an explanatory variable in DF2, the RF models showed this as the most important variable, except for the RF model of OP, where the index GNDVI is the most important. OP is a type of plant community that is distributed over patches with a high proportion of moist and bare ground (Bergamo et al., 2022), where the visible part of the spectrum (Red and Green) retrieve greater reflectance values than the far visible part of the spectrum (Red Edge and Near Infrared). The rest of the plant communities show a distribution depending on the topography, corresponding to variations in

https://doi.org/10.5194/bg-2023-95
Preprint. Discussion started: 1 August 2023

microtopography (Ward et al., 2016; Villoslada et al., 2020). Although the spatial resolution of the DEM in this study was 1 metre, it showed a similar predictive efficiency as those generated with the photogrammetric point cloud derived from UAV at a resolution below 10 cm (Villoslada et al., 2020). Overall, the results of this study show an acceptable empirical approximation to modelling the distribution of ESs providing units in large-scale images of coastal meadows of Estonia, this is, quantifying the prediction accuracy and error of PFC of small sized plant communities in heterogeneous ecosystems at a satellite spatial resolution. The methodology provides a rapid assessment of plant communities in a coastal ecosystem vulnerable to climate and land use changes using different sources of remotely sensed data. Additionally, it is shown that it is possible to reduce time and costs associated with multiple UAV flights in different areas to cover large extents by the validation of large-scale monitoring studies with open source satellite data such as Sentinel-2 and high-resolution products derived from multispectral images taken from UAV. To improve the correspondence between inter-sensor bands, it is recommended to find closer images in time with a minimum presence of clouds. Upscaling remotely sensed imagery from fine to coarse resolution is necessary, although challenging, because they provide critical information of changes needed for improved environmental management and conservation decision making at large scales. Considering this, linking UAV to Earth Observation offers the opportunity for multiscale study of environmentally sensitive ecosystems such as coastal wetlands. Further work can consider using ancillary data as a co-predictor with the aggregated spectral data, improving the prediction accuracies, as shown with DEM data in the present work. The supervised learning RF algorithm is one of the most robust ML algorithms used for ecosystem and species distribution modelling (Pichler and Hartig, 2023), however, other algorithms should be explored.

5 Conclusions

A multiscale synergy approach between UAV and Sentinel-2 MSI was undertaken in this study to model the PFC of five plant communities in coastal meadows. Good relationships existed between both sensors, which enabled PFC to be modelled using VIs, although the fusion of DEM improved the models from 1.2 to 2 times. From this research, future studies on coastal meadows using remote sensing from satellites should be focused on finding methods to achieve local calibration of the image based on values retrieved from UAV mounted multispectral cameras and thus, achieve stronger synergies between both sensors (Emilien et al, 2021). Due to the high repeat time and long duration of data collection, upscaling from UAV to satellite imagery provides an excellent resource for monitoring and assessment of the response of coastal ecosystems to loss and degradation as a result of climate change or other anthropogenic stressors. This will allow land users and managers to appropriately assess conservation priorities and implement and monitor responses.

https://doi.org/10.5194/bg-2023-95
Preprint. Discussion started: 1 August 2023

Biogeosciences Discussions
Open Access
EGU

Appendix A

A1 Additional figures and tables

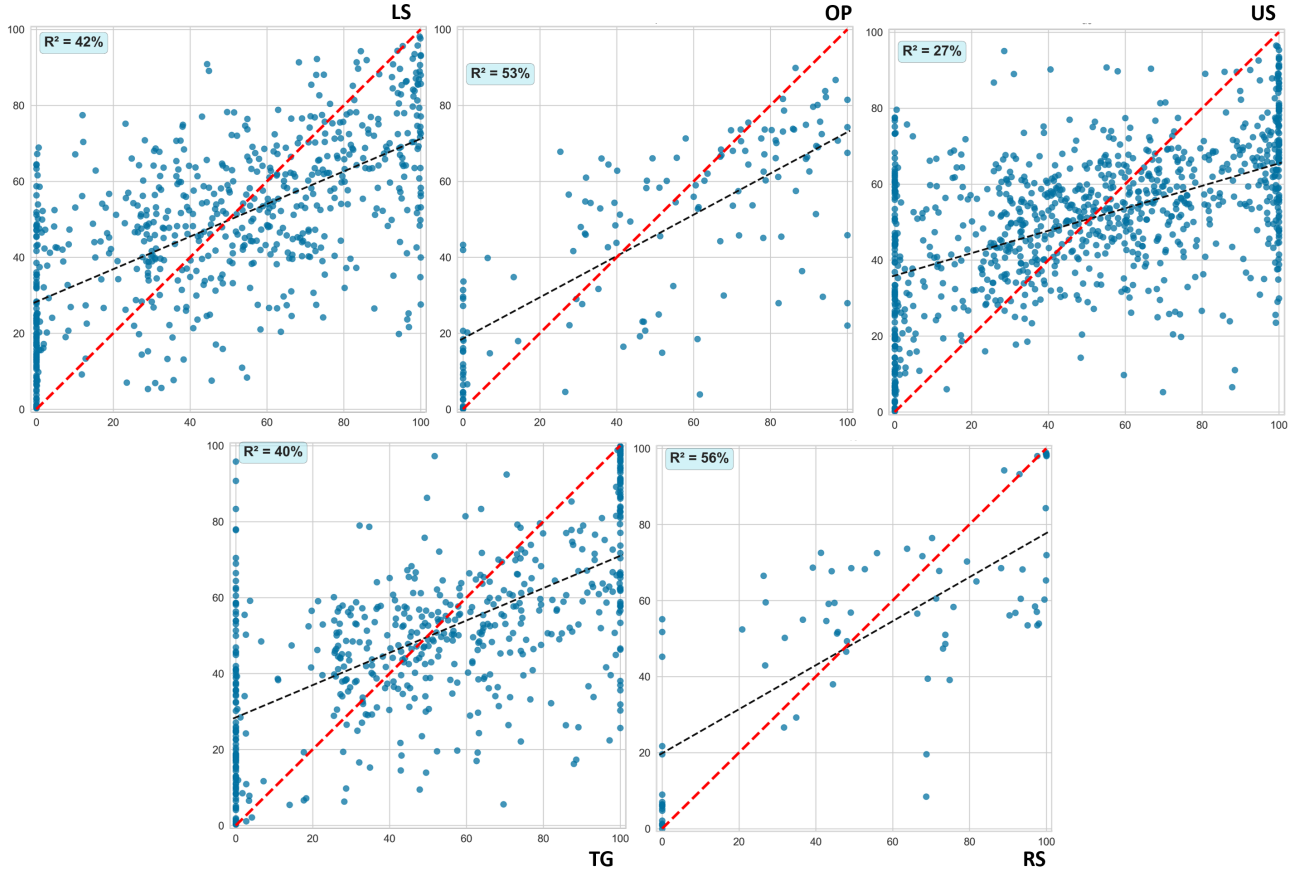

Figure A1. Prediction errors per plant community derived from RF regressions with DF1. On the x axis, actual values of Plant Fractional Cover (PFC, %) and on the y axis, predicted values of PFC (%). Black dotted lines show the best fit estimated from the correlation between the predicted and measured value of the PFC (%). Red dotted lines represent the over or under estimation of the predictions.

https://doi.org/10.5194/bg-2023-95
Preprint. Discussion started: 1 August 2023

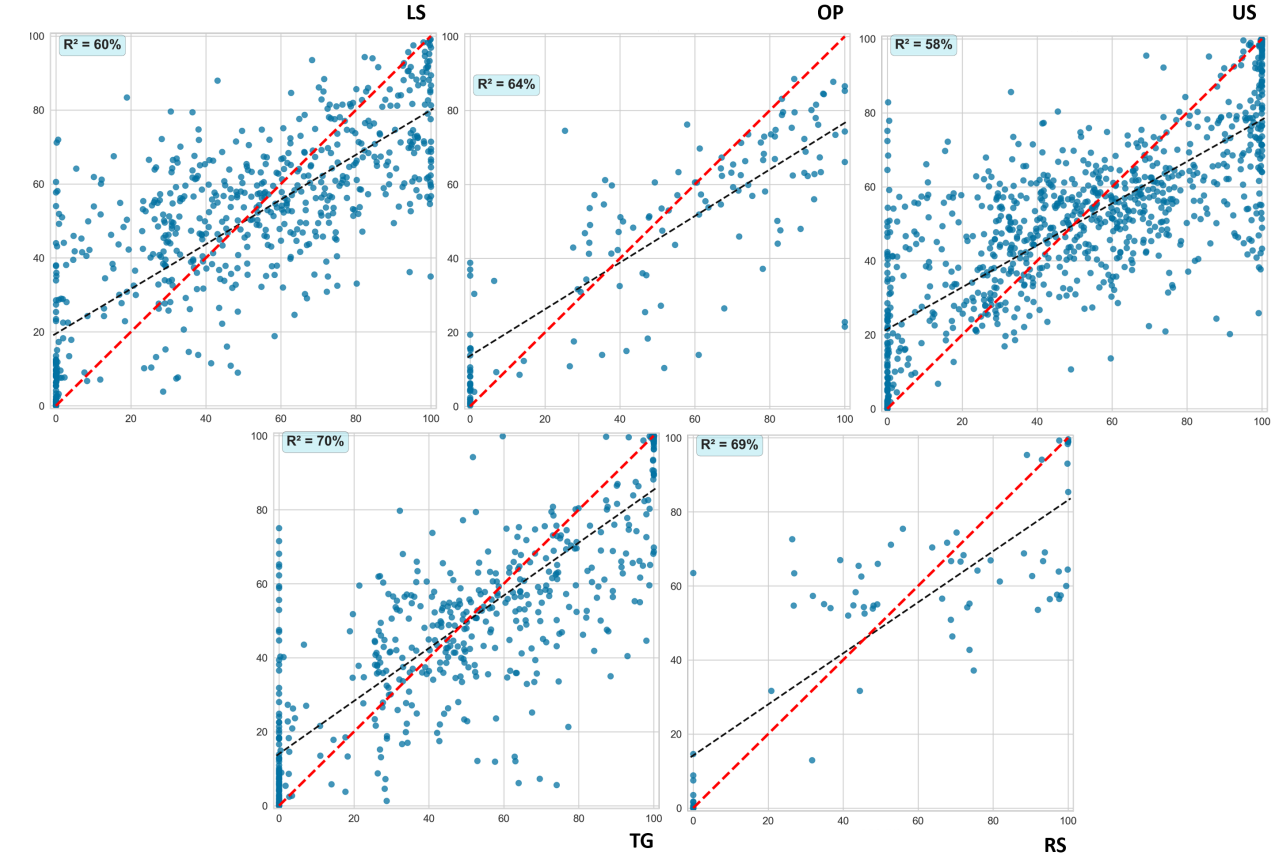

Figure A2. Prediction errors per plant community derived from RF regressions with DF2. On the x axis, actual values of Plant Fractional Cover (PFC, %) and on the y axis, predicted values of PFC (%). Black dotted lines show the best fit estimated from the correlation between the predicted and measured value of the PFC (%). Red dotted lines represent the over or under estimation of the predictions.

https://doi.org/10.5194/bg-2023-95
Preprint. Discussion started: 1 August 2023

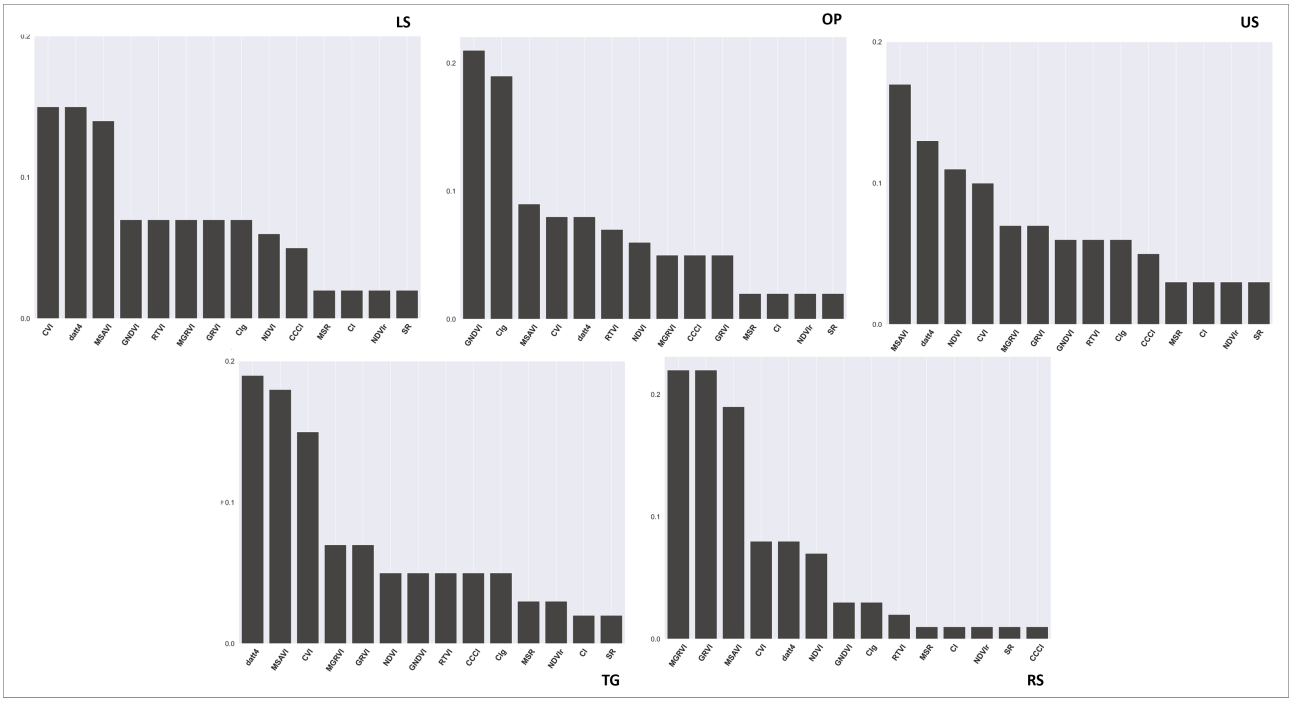

Figure A3. Variable importance retrieved by the Random Forest models derived from DF1

https://doi.org/10.5194/bg-2023-95
Preprint. Discussion started: 1 August 2023

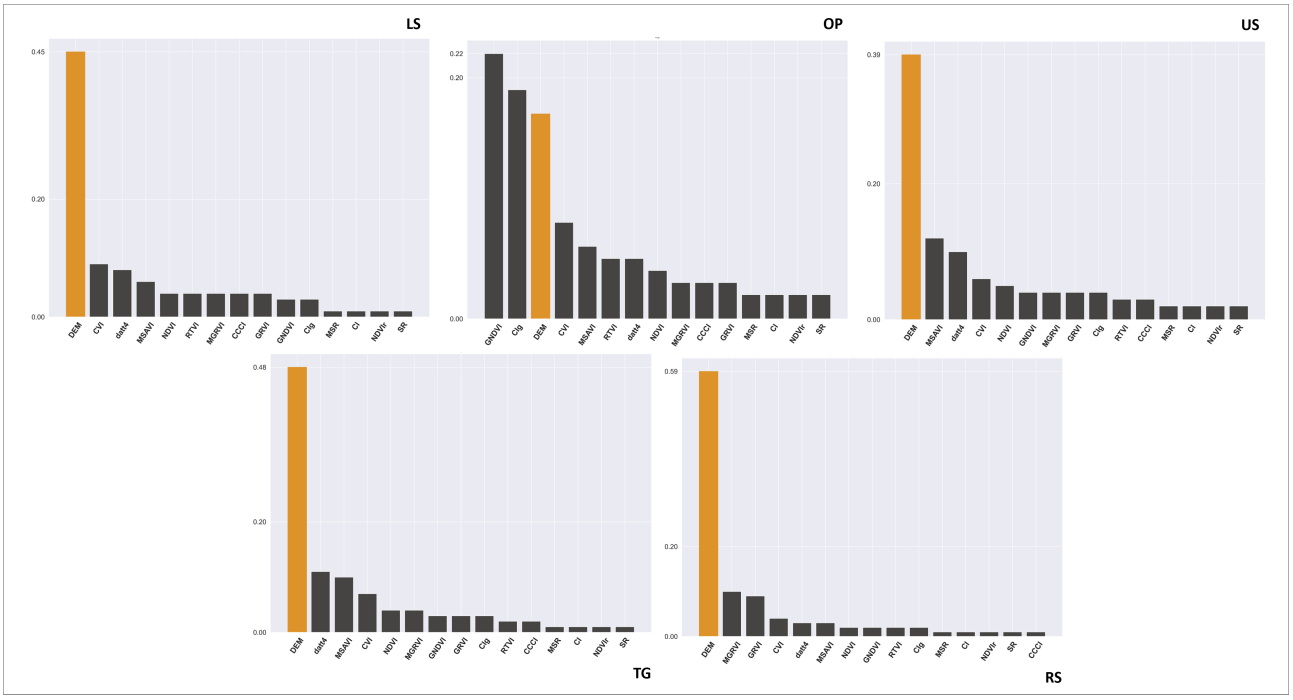

Figure A4. Variable importance retrieved by the Random Forest models derived from DF2, where the coloured bar represents the explanatory variable DEM.

Table A1. Plant communities sampled in each study area. Matsalu (MAT), Tahu South (TAS), Tahu North (TAN), Kudani (KUD), Rälby (RAL) and Rumpo (RMP); Lower Shore (LS), Open Pioneer (OP), Upper Shore (US), Tall Grass (TG), Reed Swamp (RS).

Study Area	Plant Communities
MAT	LS, OP, US, TG, RS
TAS	LS, OP, TG, US
TAN	LS, OP, US
KUD	LS, OP, TG, US
RAL	LS, OP, TG, US
RMP	LS, OP, US

https://doi.org/10.5194/bg-2023-95
Preprint. Discussion started: 1 August 2023

Author contributions. Conceptualization, R.M.P., M.V.P. and R.D.W.; methodology, R.M.P., C.B.J., M.V.P., T.F.B. and R.D.W.; software, R.M.P. and M.V.P.; validation, R.M.P., M.V.P. and R.D.W.; formal analysis, R.M.P.; investigation, R.M.P., M.V.P., T.F.B., C.B.J. and R.D.W.; resources, R.D.W. and K.S.; data curation, R.M.P., M.V.P. and R.D.W.; writing—original draft preparation, R.M.P., M.V.P. and R.D.W.; writing—review and editing, R.M.P., M.V.P., R.D.W. and C.B.J.; visualization, R.M.P.; supervision, M.V.P., R.D.W. and K.S.; project administration, R.D.W. and K.S.; funding acquisition, R.D.W. and K.S. All authors have read and agreed to the published version of the manuscript.

Competing interests. The contact author has declared that none of the authors has any competing interests.

Acknowledgements. This research was funded by the Doctoral School of Earth Sciences and Ecology, financed by the European Union, European Regional Development Fund (Estonian University of Life Sciences ASTRA project “Value-chain based bio-economy”

https://doi.org/10.5194/bg-2023-95
Preprint. Discussion started: 1 August 2023

References

European Space Agency (ESA). Copernicus Open Access Hub., https://scihub.copernicus.eu/dhus/#/home, accessed: 2022-01-30.

Eesti Maa-amet (Estonian Land Board), https://geoportaal.maaamet.ee/, accessed: 2022-03-21.

Adam, E., Mutanga, O., and Rugege, D.: Multispectral and hyperspectral remote sensing for identification and mapping of wetland vegetation: a review, Wetl. Ecol. Manag., 18, 281–296, https://doi.org/10.1007/s11273-009-9169-z, 2010.

Andreatta, D., Gianelle, D., Scotton, M., and Dalponte, M.: Estimating grassland vegetation cover with remote sensing: A comparison between Landsat-8, Sentinel-2 and PlanetScope imagery, Ecol. Indic., 141, 109 102, https://doi.org/https://doi.org/10.1016/j.ecolind.2022.109102, 2022.

Barnes, E., Clarke, T., Richards, S., Colaizzi, P., Haberland, J., Kostrzewski, M., Waller, P., Choi, C., Riley, E., and Thompson, T.: Coincident detection of crop water stress, nitrogen status and canopy density using ground-based multispectral data, in: Proc. 5th Int. Conf. Precis. Agric. Resour. Manag., Bloomington, MN USA, 2000.

Bendig, J., Yu, K., Aasen, H., Bolten, A., Bennertz, S., Broscheit, J., Gnyp, M. L., and Bareth, G.: Combining UAV-based plant height from crop surface models, visible, and near infrared vegetation indices for biomass monitoring in barley, Int. J. Appl. Earth. Obs., 39, 79–87, https://doi.org/https://doi.org/10.1016/j.jag.2015.02.012, 2015.

Berg, M., Joyce, C., and Burnside, N.: Differential responses of abandoned wet grassland plant communities to reinstated cutting management, Hydrobiologia, 692, 83–97, https://doi.org/10.1007/s10750-011-0826-x, 2012.

Bergamo, T. F., Ward, R. D., Joyce, C. B., Villoslada, M., and Sepp, K.: Experimental climate change impacts on Baltic coastal wetland plant communities, Sci.Rep-UK, 12, 20 362, https://doi.org/10.1038/s41598-022-24913-z, 2022.

Bergamo, T. F., de Lima, R. S., Kull, T., Ward, R. D., Sepp, K., and Villoslada, M.: From UAV to PlanetScope: Upscaling fractional cover of an invasive species Rosa rugosa, J. of Environ. Manage., 336, 117 693, https://doi.org/https://doi.org/10.1016/j.jenvman.2023.117693, 2023.

Brodu, N.: Super-Resolving Multiresolution Images With Band-Independent Geometry of Multispectral Pixels, IEEE T. Geosci. Remote., 55, 4610–4617, https://doi.org/10.1109/TGRS.2017.2694881, 2017.

Burkhard, B., Kroll, F., Nedkov, S., and Müller, F.: Mapping ecosystem service supply, demand and budgets, Ecol. Indic., 21, 17–29, https://doi.org/https://doi.org/10.1016/j.ecolind.2011.06.019, challenges of sustaining natural capital and ecosystem services, 2012.

Burnside, N., Joyce, C., Puurmann, E., and Scott, D.: Use of vegetation classification and plant indicators to assess grazing abandonment in Estonian coastal wetlands, J. Veg. Sci., 18, 645–654, https://doi.org/10.1111/j.1654-1103.2007.tb02578.x, 2007.

Chen, A., Orlov-Levin, V., and Meron, M.: Applying high-resolution visible-channel aerial imaging of crop canopy to precision irrigation management, Agr. Water Manage., 216, 196–205, https://doi.org/https://doi.org/10.1016/j.agwat.2019.02.017, 2019.

Chen, P.-F., Nicolas, T., Wang, J.-H., Philippe, V., Huang, W.-J., and Li, B.-G.: New index for crop canopy fresh biomass estimation, Spectrosc. Spect. Anal., 30, 512–517, 2010.

Chytry, M., Schaminée, J., and Schwabe, A.: Vegetation survey: A new focus for Applied Vegetation Science, Applied Vegetation Science, 14, 435–439, https://doi.org/10.1111/j.1654-109X.2011.01154.x, 2011.

Colomina, I. and Molina, P.: Unmanned aerial systems for photogrammetry and remote sensing: A review, ISPRS J. Photogramm., 92, 79–97, https://doi.org/https://doi.org/10.1016/j.isprsjprs.2014.02.013, 2014.

Corbane, C., Lang, S., Pipkins, K., Alleaume, S., Deshayes, M., García Millán, V. E., Strasser, T., Vanden Borre, J., Toon, S., and Michael, F.: Remote sensing for mapping natural habitats and their conservation status – New opportunities and challenges, Int. J. Appl. Earth. Obs.,

https://doi.org/10.5194/bg-2023-95
Preprint. Discussion started: 1 August 2023

37, 7–16, https://doi.org/https://doi.org/10.1016/j.jag.2014.11.005, special Issue on Earth observation for habitat mapping and biodiversity monitoring, 2015.

Courouble, M.: Global Wetland Outlook: Special Edition 2021, Secretariat of the Convention on Wetlands, Gland, Switzerland, 2021.

Cracknell, A. P.: UAVs: regulations and law enforcement, Int. J. Remote Sens., 38, 3054–3067, https://doi.org/10.1080/01431161.2017.1302115, 2017.

Datt, B.: Remote Sensing of Chlorophyll a, Chlorophyll b, Chlorophyll a+b, and Total Carotenoid Content in Eucalyptus Leaves, Remote Sens. Environ., 66, 111–121, https://doi.org/https://doi.org/10.1016/S0034-4257(98)00046-7, 1998.

Davidson, N.: How much wetland has the world lost? Long-term and recent trends in global wetland area, Mar. Freshwater Res., 65, 936–941, https://doi.org/10.1071/MF14173, 2014.

De Simone, W., Allegrezza, M., Frattaroli, A. R., Montecchiari, S., Tesei, G., Zuccarello, V., and Di Musciano, M.: From Remote Sensing to Species Distribution Modelling: An Integrated Workflow to Monitor Spreading Species in Key Grassland Habitats, Remote Sens., 13, https://doi.org/10.3390/rs13101904, 2021.

Díaz-Delgado, R., Cazacu, C., and Adamescu, M.: Rapid Assessment of Ecological Integrity for LTER Wetland Sites by Using UAV Multispectral Mapping, Drones, 3, https://doi.org/10.3390/drones3010003, 2019a.

Díaz-Delgado, R., Cazacu, C., and Adamescu, M.: Rapid Assessment of Ecological Integrity for LTER Wetland Sites by Using UAV Multispectral Mapping, Drones, 3, https://doi.org/10.3390/drones3010003, 2019b.

Emilien, A.-V., Thomas, C., and Houet, T.: UAV & Satellite synergies for optical remote sensing applications: a literature review, Sci. Remote Sens., 3, 100 019, https://doi.org/10.1016/j.srs.2021.100019, 2021.

ESA: SNAP.ESA Sentinel Application Platform v9, http://step.esa.int., 2014.

Evans, J. S., Murphy, M. A., Holden, Z. A., and Cushman, S. A.: Modeling Species Distribution and Change Using Random Forest, pp. 139–159, Springer New York, New York, NY, https://doi.org/10.1007/978-1-4419-7390-0_8, 2011.

E Thessen, A.: Adoption of Machine Learning Techniques in Ecology and Earth Science, One Ecosyst., 1, e8621, https://doi.org/10.3897/oneeco.1.e8621, 2016.

Fawcett, D., Panigada, C., Tagliabue, G., Boschetti, M., Celesti, M., Evdokimov, A., Biriukova, K., Colombo, R., Miglietta, F., Rascher, U., and Anderson, K.: Multi-Scale Evaluation of Drone-Based Multispectral Surface Reflectance and Vegetation Indices in Operational Conditions, Remote Sens., 12, https://doi.org/10.3390/rs12030514, 2020.

Fernández-Guisuraga, J. M., Sanz-Ablanedo, E., Suárez-Seoane, S., and Calvo, L.: Using Unmanned Aerial Vehicles in Post-fire Vegetation Survey Campaigns through Large and Heterogeneous Areas: Opportunities and Challenges, Sensors, 18, https://doi.org/10.3390/s18020586, 2018.

Ferreira, B., Silva, R. G., and Iten, M.: Earth Observation Satellite Imagery Information Based Decision Support Using Machine Learning, Remote Sens., 14, https://doi.org/10.3390/rs14153776, 2022.

Findell, K. L., Berg, A., Gentine, P., Krasting, J. P., Lintner, B. R., Malyshev, S., Santanello, J. A., and Shevliakova, E.: The impact of anthropogenic land use and land cover change on regional climate extremes, Nat. Commun., 8, 989, https://doi.org/10.1038/s41467-017-01038-w, 2017.

Gardner, T. A., Barlow, J., Chazdon, R., Ewers, R. M., Harvey, C. A., Peres, C. A., and Sodhi, N. S.: Prospects for tropical forest biodiversity in a human-modified world, Ecol. Lett., 12, 561–582, 2009.

Gedan, K., Kirwan, M., Wolanski, E., Barbier, E., and Silliman, B.: The Present and Future Role of Coastal Wetland Vegetation in Protecting Shorelines: Answering Recent Challenges to the Paradigm, Clim. Change, 106, 7–29, https://doi.org/10.1007/s10584-010-0003-7, 2011.

https://doi.org/10.5194/bg-2023-95
Preprint. Discussion started: 1 August 2023

Gillies, S.: Rasterio: geospatial raster I/O for Python programmers, https://github.com/mapbox/rasterio, 2013.

Gitelson, A. and Merzlyak, M. N.: Spectral Reflectance Changes Associated with Autumn Senescence of Aesculus hippocastanum L. and Acer platanoides L. Leaves. Spectral Features and Relation to Chlorophyll Estimation, J. Plant Physiol., 143, 286–292, https://doi.org/https://doi.org/10.1016/S0176-1617(11)81633-0, 1994.

Gitelson, A., Viña, A., Arkebauer, T., Rundquist, D., Keydan, G., Leavitt, B., and Keydan, G.: Remote estimation of leaf area index and green leaf biomass in maize canopies, Geophys. Res. Lett., 30, 1248, https://doi.org/10.1029/2002GL016450, 2003.

Gitelson, A. A., Kaufman, Y. J., and Merzlyak, M. N.: Use of a green channel in remote sensing of global vegetation from EOS-MODIS, Remote Sens. Environ., 58, 289–298, https://doi.org/https://doi.org/10.1016/S0034-4257(96)00072-7, 1996.

Harris, C. R., Millman, K. J., van der Walt, S. J., Gommers, R., Virtanen, P., Cournapeau, D., Wieser, E., Taylor, J., Berg, S., Smith, N. J., Kern, R., Picus, M., Hoyer, S., van Kerkwijk, M. H., Brett, M., Haldane, A., del Río, J. F., Wiebe, M., Peterson, P., Gérard-Marchant, P., Sheppard, K., Reddy, T., Weckesser, W., Abbasi, H., Gohlke, C., and Oliphant, T. E.: Array programming with NumPy, Nature, 585, 357–362, https://doi.org/10.1038/s41586-020-2649-2, 2020.

Heil, J., Jörges, C., and Stumpe, B.: Fine-Scale Mapping of Soil Organic Matter in Agricultural Soils Using UAVs and Machine Learning, Remote Sens., 14, https://doi.org/10.3390/rs14143349, 2022.

Hopkinson, C. S., Cai, W.-J., and Hu, X.: Carbon sequestration in wetland dominated coastal systems—a global sink of rapidly diminishing magnitude, Curr. Opin. Env. Sust., 4, 186–194, https://doi.org/https://doi.org/10.1016/j.cosust.2012.03.005, carbon and nitrogen cycles, 2012.

Isenburg, M., Liu, Y., Shewchuk, J., Snoeyink, J., and Thirion, T.: Generating Raster DEM from Mass Points Via TIN Streaming, pp. 186–198, https://doi.org/10.1007/11863939_13, 2006.

Isgró, M. A., Basallote, M. D., Caballero, I., and Barbero, L.: Comparison of UAS and Sentinel-2 Multispectral Imagery for Water Quality Monitoring: A Case Study for Acid Mine Drainage Affected Areas (SW Spain), Remote Sens., 14, https://doi.org/10.3390/rs14164053, 2022.

Jiang, J., Johansen, K., Tu, Y.-H., and McCabe, M.: Multi-sensor and multi-platform consistency and interoperability between UAV, Planet CubeSat, Sentinel-2, and Landsat reflectance data, GIScience Remote sens., 59, 936–958, https://doi.org/10.1080/15481603.2022.2083791, 2022.

Jordahl, K., den Bossche, J. V., Fleischmann, M., Wasserman, J., McBride, J., Gerard, J., Tratner, J., Perry, M., Badaracco, A. G., Farmer, C., Hjelle, G. A., Snow, A. D., Cochran, M., Gillies, S., Culbertson, L., Bartos, M., Eubank, N., maxalbert, Bilogur, A., Rey, S., Ren, C., Arribas-Bel, D., Wasser, L., Wolf, L. J., Journois, M., Wilson, J., Greenhall, A., Holdgraf, C., Filipe, and Leblanc, F.: geopandas/geopandas: v0.8.1, https://doi.org/10.5281/zenodo.3946761, 2020.

Knight, J. F., Lunetta, R. S., Ediriwickrema, J., and Khorram, S.: Regional Scale Land Cover Characterization Using MODIS-NDVI 250 m Multi-Temporal Imagery: A Phenology-Based Approach, GIScience Remote sens., 43, 1–23, https://doi.org/10.2747/1548-1603.43.1.1, 2006.

Laliberte, A. S., Goforth, M. A., Steele, C. M., and Rango, A.: Multispectral Remote Sensing from Unmanned Aircraft: Image Processing Workflows and Applications for Rangeland Environments, Remote Sens., 3, 2529–2551, https://doi.org/10.3390/rs3112529, 2011.

Lima-Cueto, F. J., Blanco-Sepúlveda, R., Gómez-Moreno, M. L., and Galacho-Jiménez, F. B.: Using Vegetation Indices and a UAV Imaging Platform to Quantify the Density of Vegetation Ground Cover in Olive Groves (Olea Europaea L.) in Southern Spain, Remote Sens., 11, https://doi.org/10.3390/rs11212564, 2019.

https://doi.org/10.5194/bg-2023-95
Preprint. Discussion started: 1 August 2023

Luck, G., Daily, G., and Ehrlich, P.: Population diversity and ecosystem services, Trends Ecol. Evol., 18, 331–336, https://doi.org/10.1016/S0169-5347(03)00100-9, 2003.

Magurran, A. E.: Ecological Diversity and Its Measurement, Princeton University Press, Princeton, New Jersey, 1988.

Mahdianpari, M., Granger, J. E., Mohammadimanesh, F., Salehi, B., Brisco, B., Homayouni, S., Gill, E., Huberty, B., and Lang, M.: Meta-Analysis of Wetland Classification Using Remote Sensing: A Systematic Review of a 40-Year Trend in North America, Remote Sens., 12, https://doi.org/10.3390/rs12111882, 2020.

Main-Knorn, M., Pflug, B., Louis, J., Debaecker, V., Müller-Wilm, U., and Gascon, F.: Sen2Cor for Sentinel-2, in: Image and Signal Processing for Remote Sensing XXIII, edited by Bruzzone, L., vol. 10427, p. 1042704, International Society for Optics and Photonics, SPIE, https://doi.org/10.1117/12.2278218, 2017.

Mao, P., Ding, J., Jiang, B., Qin, L., and Qiu, G. Y.: How can UAV bridge the gap between ground and satellite observations for quantifying the biomass of desert shrub community?, ISPRS J. Photogramm., 192, 361–376, https://doi.org/https://doi.org/10.1016/j.isprsjprs.2022.08.021, 2022.

Martínez Prentice, R., Villoslada Peciña, M., Ward, R. D., Bergamo, T. F., Joyce, C. B., and Sepp, K.: Machine Learning Classification and Accuracy Assessment from High-Resolution Images of Coastal Wetlands, Remote Sens., 13, https://doi.org/10.3390/rs13183669, 2021.

Maurya, A., Nadeem, M., Singh, D., Singh, K., and Rajput, N.: Critical Analysis of Machine Learning Approaches for Vegetation Fractional Cover Estimation Using Drone and Sentinel-2 Data, pp. 343–346, https://doi.org/10.1109/IGARSS47720.2021.9554422, 2021.

Maxwell, A. E., Warner, T. A., and Fang, F.: Implementation of machine-learning classification in remote sensing: an applied review, Int. J. Remote Sens., 39, 2784–2817, https://doi.org/10.1080/01431161.2018.1433343, 2018.

McKinney, W.: Data Structures for Statistical Computing in Python, pp. 56–61, https://doi.org/10.25080/Majora-92bf1922-00a, 2010.

Merzlyak, M. N., Gitelson, A. A., Chivkunova, O. B., Solovchenko, A. E., and Pogosyan, S. I.: Application of Reflectance Spectroscopy for Analysis of Higher Plant Pigments, Russ. J. Plant. Physl+, 50, 704–710, https://doi.org/10.1023/A:1025608728405, 2003.

Muukkonen, P. and Heiskanen, J.: Biomass estimation over a large area based on standwise forest inventory data and ASTER and MODIS satellite data: A possibility to verify carbon inventories, Remote Sens. Environ., 107, 617–624, https://doi.org/https://doi.org/10.1016/j.rse.2006.10.011, 2007.

Okolie, C. J. and Smit, J. L.: A systematic review and meta-analysis of Digital elevation model (DEM) fusion: pre-processing, methods and applications, ISPRS J. Photogramm., 188, 1–29, https://doi.org/https://doi.org/10.1016/j.isprsjprs.2022.03.016, 2022.

Olden, J. D., Lawler, J. J., and Poff, N. L.: Machine learning methods without tears: a primer for ecologists, Q Rev Biol., 83, 171–193, 2008.

Padró, J.-C., Muñoz, F.-J., Ávila, L. , Pesquer, L., and Pons, X.: Radiometric Correction of Landsat-8 and Sentinel-2A Scenes Using Drone Imagery in Synergy with Field Spectroradiometry, Remote Sens., 10, https://doi.org/10.3390/rs10111687, 2018.

Pedregosa, F., Varoquaux, G., Gramfort, A., Michel, V., Thirion, B., Grisel, O., Blondel, M., Müller, A., Nothman, J., Louppe, G., Prettenhofer, P., Weiss, R., Dubourg, V., Vanderplas, J., Passos, A., Cournapeau, D., Brucher, M., Perrot, M., and Édouard Duchesnay: Scikit learn: Machine Learning in Python, 2018.

Pettorelli, N., Laurance, W. F., O'Brien, T. G., Wegmann, M., Nagendra, H., and Turner, W.: Satellite remote sensing for applied ecologists: opportunities and challenges, J Appl. Ecol., 51, 839–848, https://doi.org/https://doi.org/10.1111/1365-2664.12261, 2014.

Pichler, M. and Hartig, F.: Machine learning and deep learning—A review for ecologists, Methods Ecol. Evol., 14, 994–1016, https://doi.org/10.1111/2041-210x.14061, 2023.

Probst, P., Wright, M. N., and Boulesteix, A.-L.: Hyperparameters and tuning strategies for random forest, Data Min. Knowl. Disc., 9, https://doi.org/10.1002/widm.1301, 2019.

https://doi.org/10.5194/bg-2023-95
Preprint. Discussion started: 1 August 2023

Qi, J., Chehbouni, A., Huete, A., Kerr, Y., and Sorooshian, S.: A modified soil adjusted vegetation index, Remote Sens. Environ., 48, 119–126, https://doi.org/https://doi.org/10.1016/0034-4257(94)90134-1, 1994.

Rannap, R., Briggs, L., Lotman, K., Lepik, I., Rannap, V., and Põdra, P.: Coastal Meadow Management—Best Practice Guidelines, vol. 4, Ministry of the Environment of the Republic of Estonia, 2004.

Riihimäki, H., Luoto, M., and Heiskanen, J.: Estimating fractional cover of tundra vegetation at multiple scales using unmanned aerial systems and optical satellite data, Remote Sens. Environ., 224, 119–132, https://doi.org/https://doi.org/10.1016/j.rse.2019.01.030, 2019.

Rivis, R., Kont, A., Ratas, U., Palginomm, V., Antso, K., and Tõnisson, H.: Trends in the development of Estonian coastal land cover and landscapes caused by natural changes and human impact, J. Coast. Conserv., 20, 199–209, https://doi.org/10.1007/s11852-016-0430-3, 2016.

Rodriguez-Galiano, V., Ghimire, B., Rogan, J., Chica-Olmo, M., and Rigol-Sanchez, J.: An assessment of the effectiveness of a random forest classifier for land-cover classification, ISPRS J. Photogramm., 67, 93–104, https://doi.org/https://doi.org/10.1016/j.isprsjprs.2011.11.002, 2012.

Rouse, J. W., Haas, R. H., Schell, J. A., and Deering, D. W.: Monitoring vegetation systems in the great plains with ERTS, 1973.

Schuster, C., Förster, M., and Kleinschmit, B.: Testing the red edge channel for improving land-use classifications based on high-resolution multi-spectral satellite data, Int. J. Remote Sens., 33, 5583–5599, https://doi.org/10.1080/01431161.2012.666812, 2012.

Shiferaw, H., Bewket, W., and Eckert, S.: Performances of machine learning algorithms for mapping fractional cover of an invasive plant species in a dryland ecosystem, Ecol. Evol., 9, 2562–2574, 2019.

Spiegelberger, T., Gillet, F., Amiaud, B., Thébault, A., Mariotte, P., and Buttler, A.: How do plant community ecologists consider the complementarity of observational, experimental and theoretical modelling approaches?, Plant Ecol. Evol., 145, 4–12, https://doi.org/10.5091/plecevo.2012.699, 2012.

Sutton-Grier, A. E. and Sandifer, P. A.: Conservation of Wetlands and Other Coastal Ecosystems: a Commentary on their Value to Protect Biodiversity, Reduce Disaster Impacts, and Promote Human Health and Well-Being, Wetlands, 39, 1295–1302, https://doi.org/10.1007/s13157-018-1039-0, 2019.

Tang, B., Frye, H. A., Gelfand, A. E., and Silander, J. A.: Zero-Inflated Beta Distribution Regression Modeling, JABES, 28, 117–137, https://doi.org/https://doi.org/10.1007/s13253-022-00516-z, 2023.

Turpie, K.: Explaining the Spectral Red-Edge Features of Inundated Marsh Vegetation, J. Coast. Res., 29, 1111–1117, https://doi.org/10.2112/JCOASTRES-D-12-00209.1, 2013.

Valavi, R., Elith, J., Lahoz-Monfort, J., and Guillera-Arroita, G.: Modelling species presence-only data with random forests, Ecography, 44, https://doi.org/10.1111/ecog.05615, 2021.

Van der Maarel, E.: Vegetation ecology, Blackwell Science Ltd, Oxford, 2005.

Villoslada, M., Bergamo, T., Ward, R., Burnside, N., Joyce, C., Bunce, R., and Sepp, K.: Fine scale plant community assessment in coastal meadows using UAV based multispectral data, Ecol. Indic., 111, 105 979, https://doi.org/https://doi.org/10.1016/j.ecolind.2019.105979, 2020.

Villoslada Peciña, M., Bergamo, T., Ward, R., Joyce, C., and Sepp, K.: A novel UAV-based approach for biomass prediction and grassland structure assessment in coastal meadows, Ecol. Indic., 122, 107 227, https://doi.org/https://doi.org/10.1016/j.ecolind.2020.107227, 2021.

Vincini, M., Frazzi, E., and D'Alessio, P.: A broad-band leaf chlorophyll vegetation index at the canopy scale, Precis. Agric., 9, 303–319, https://doi.org/10.1007/s11119-008-9075-z, 2008.

https://doi.org/10.5194/bg-2023-95
Preprint. Discussion started: 1 August 2023

Ward, R., Burnside, N., Joyce, C., and Sepp, K.: The use of medium point density LiDAR elevation data to determine plant community types in Baltic coastal wetlands, Ecol. Indic., 33, 96–104, https://doi.org/10.1016/j.ecolind.2012.08.016, 2013.

Ward, R., Burnside, N., Joyce, C., and Sepp, K.: Importance of Microtopography in Determining Plant Community Distribution in Baltic Coastal Wetlands, J. Coast. Res., 32, 1062–1070, https://doi.org/10.2112/JCOASTRES-D-15-00065.1, 2016.

Ward, R. D.: Carbon sequestration and storage in Norwegian Arctic coastal wetlands: Impacts of climate change, Sci. of The Total Environ., 748, 141 343, https://doi.org/https://doi.org/10.1016/j.scitotenv.2020.141343, 2020.

Wu, C., Niu, Z., Tang, Q., and Huang, W.: Estimating chlorophyll content from hyperspectral vegetation indices: Modeling and validation, Agr. Forest Meteorol., 148, 1230–1241, https://doi.org/https://doi.org/10.1016/j.agrformet.2008.03.005, 2008.

Zabala, S.: Comparison of Multi-Temporal and Multispectral Sentinel-2 and Unmanned Aerial Vehicle Imagery for Crop Type Mapping, Master's thesis, Lund University, Lund, Sweden, 2017.

Zhang, L., Huettmann, F., Zhang, X., Liu, S., Sun, P., Yu, Z., and Mi, C.: The use of classification and regression algorithms using the random forests method with presence-only data to model species' distribution, MethodsX, 6, 2281–2292, https://doi.org/https://doi.org/10.1016/j.mex.2019.09.035, 2019.

Zhu, W., Rezaei, E. E., Nouri, H., Yang, T., Li, B., Gong, H., Lyu, Y., Peng, J., and Sun, Z.: Quick Detection of Field-Scale Soil Comprehensive Attributes via the Integration of UAV and Sentinel-2B Remote Sensing Data, Remote Sens., 13, https://doi.org/10.3390/rs13224716, 2021.